forests

MDPI

Article

Applications of TLS and ALS in Evaluating Forest Ecosystem Services: A Southern Carpathians Case Study

Alexandru Claudiu Dobre [1,2], Ionuț-Silviu Pascu [1,2,*], Ștefan Leca [2], Juan Garcia-Duro [2], Carmen-Elena Dobrota [3,4], Gheorghe Marian Tudoran [1] and Ovidiu Badea [1,2]

1 Department of Forest Engineering, Forest Management Planning and Terrestrial Measurements, Faculty of Silviculture and Forest Engineering, "Transilvania" University, 1 Ludwig van Beethoven Str., 500123 Brașov, Romania; dobre.alexandruclaudiu@gmail.com (A.C.D.); tudoran.george@unitbv.ro (G.M.T.); ovidiu.badea63@gmail.com (O.B.)
2 Development in Forestry-Department of Forest Monitoring, "Marin Drăcea" Romanian National Institute for Research, 128 Eroilor Blvd., 077190 Voluntari, Romania; stefan.leca@icas.ro (Ș.L.); juan.garcia.duro@icas.ro (J.G.-D.)
3 Faculty of Business and Administration, University of Bucharest, 4-12 B-dul Regina Elisabeta, County 3, 030018 Bucharest, Romania; dobrotacarmen@yahoo.com
4 Institute of National Economy, Romanian Academy, 13 Calea 13 Septembrie, County 5, 050726 Bucharest, Romania
* Correspondence: ionut.pascu@icas.ro; Tel.: +40-7-2633-2258

Abstract: Forests play an important role in biodiversity conservation, being one of the main providers of ecosystem services, according to the Economics of Ecosystems and Biodiversity. The functions and ecosystem services provided by forests are various concerning the natural capital and the socio-economic systems. Past decades of remote-sensing advances make it possible to address a large set of variables, including both biophysical parameters and ecological indicators, that characterize forest ecosystems and their capacity to supply services. This research aims to identify and implement existing methods that can be used for evaluating ecosystem services by employing airborne and terrestrial stationary laser scanning on plots from the Southern Carpathian mountains. Moreover, this paper discusses the adaptation of field-based approaches for evaluating ecological indicators to automated processing techniques based on airborne and terrestrial stationary laser scanning (ALS and TLS). Forest ecosystem functions, such as provisioning, regulation, and support, and the overall forest condition were assessed through the measurement and analysis of stand-based biomass characteristics (e.g., trees' heights, wood volume), horizontal structure indices (e.g., canopy cover), and recruitment-mortality processes as well as overall health status assessment (e.g., dead trees identification, deadwood volume). The paper, through the implementation of the above-mentioned analyses, facilitates the development of a complex multi-source monitoring approach as a potential solution for assessing ecosystem services provided by the forest, as well as a basis for further monetization approaches.

Keywords: ecosystem services; natural capital; socio-economic system; ecological indicators; terrestrial laser scanning; aerial laser scanning

Citation: Dobre, A.C.; Pascu, I.-S.; Leca, Ș.; Garcia-Duro, J.; Dobrota, C.-E.; Tudoran, G.M.; Badea, O. Applications of TLS and ALS in Evaluating Forest Ecosystem Services: A Southern Carpathians Case Study. *Forests* **2021**, *12*, 1269. https://doi.org/10.3390/f12091269

Academic Editor: Jarosław Socha

Received: 20 August 2021
Accepted: 13 September 2021
Published: 17 September 2021

1. Introduction

Forest is playing a crucial role in biological diversity, local welfare, the balance of carbon emissions, and the global economy [1–3]. In the context of climate change, the understanding of forest ecosystem processes' importance is essential in assuring sustainable management and economic development [4]. Toward this purpose, forest monitoring was established as the main tool for studying the dynamics of forest structure and functioning and its response to anthropogenic influences [3,5]. The necessity of this tool is highlighted by decisional factors' requirements and forest governance [6]. Due to the high

complexity of the forest dynamics, a high amount of warranted information is needed in the characterization process.

The primary mechanism of forest monitoring in assuring the data integration is developing forest inventories focused on parameters related to the main dendrometric characteristics of trees (e.g., diameter at breast height (DBH), height-DBH ratio, crown width). Besides these variables, the monitoring also has to take into consideration information regarding the climate (temperature and precipitations) and pollution (atmospheric depositions). However, it is a well-known fact that the traditional forest inventory can be expensive, time-consuming, and requires a large amount of qualified personnel [3]. Moreover, forest inventory is limited to statistically established sample plots, resulting in a weaker representativity at larger scales [7–9].

To overcome the mentioned limitations, alternative solutions and measuring methodologies were sought in the remote-sensing field. In the past decades, remote-sensing systems have evolved, ensuring a large variety of applications [10]. As expected, the remote-sensing portfolio already contains several techniques addressing forest ecology and management [11]. From their beginning, remote-sensing systems were mostly equivalated to satellite imagery. New instruments of interest here, airborne laser scanning, unmanned aerial vehicles, digital photography systems, and terrestrial laser scanners, have more recently captured the researchers' attention, gradually gaining visibility through a large number of scientific studies.

Land cover analysis [12,13], biomass estimation [14–17], hazard identification [18–20], structure assessment [21–26], and ecological indicators are just some of the most frequent applications of remote sensing in forestry. The major advantages of remote sensing are related to its capability of capturing a large amount of data and the possibility of revisiting in relatively short periods, as well as the plurality of the associated analyses [24].

A keen interest in remote sensing was shown toward biophysical parameters, such as DBH, tree height, volume, and implicitly biomass. The majority of these parameters were initially computed employing regression models, with input data derived from crown projections and height measurements from passive sensors [27–29], calibrated with ground samples. New technologies, as is the case of terrestrial laser scanning, propose different approaches for estimating tree characteristics. These provide a more direct method that involves point cloud classification, tree segmentation, and stem reconstruction [30–32]. Besides the biophysical parameters, active remote-sensing systems are used to describe stands' structure through indirect analyses of the number of trees, canopy stratification, and trees distribution. As described in the work of [24,33,34], airborne and terrestrial laser scanning represent optimal solutions in describing forest stands through structural indicators based on point cloud processing.

Regarding this matter, the literature offers a rich variety of active remote-sensing-based forest variables, from foliage indices [24,35,36] (leaf area index—LAI, gap probability—p_{gap}) to trees spatial distribution [37,38] (mostly distance and angles between trees, but also the position itself for marginal trees detection, sampling plot edge effect mitigation, etc.). Satellite imagery also proposes indicators related to the status of forest stand health [39–42], an aspect that will not be detailed here since passive remote sensing does not make the subject of our study.

Disregarding the plethora of variables and its promising evolution, passive remote-sensing technology still demands innovative approaches to address the requirements of ecological relevant indicators [11]. The constant need for ground measurement calibration represents the main disadvantage of most passive remote-sensing systems. Furthermore, the applications based on regression models can lead to important errors due to potentially incorrect assumptions regarding the relationship between forest characteristics [43,44].

In the ecological research field, active remote-sensing data are increasingly being used. Quantifying forest ecosystems information from indices based on active remote-sensing highlights the need for further analysis and adaptation. The processing and uptake of these data are necessary for linking the indicators to the capacity of forest ecosystems to provide

benefits. These benefits materialize in what we call ecosystem services and represent the ecosystems' benefits, processes, and assets for providing human well-being [45].

In the field of research, the relationship between ecology and economy has been attributed with great importance, a fact that is corroborated by the very nature of ecosystem services. This has made it possible to develop the concept of natural capital on an environmental basis [46] and led to the idea of value, from a monetary point of view, of the ecosystem services and goods [47]. The need to exploit the benefits of ecosystems derives from their contribution to the human economy [48,49] and their expression in services and commercial goods [50,51].

Nowadays, there is a multitude of methods for evaluating and monetizing services, most of them being subjective. The methods are based on human preferences or physical costs upon which ecosystem services can be integrated [46]. The established methods are based on damaged cost avoided, replacement cost, market price, productivity cost, hedonic pricing, benefits transfer, and contingent evaluation method [51–53].

Despite the difficulties encountered in the process of applying ecosystem evaluation methods, they have an essential role in communicating the value of nature to the decisional factors and policymakers [54]. In this regard, there is an absolute need for objective ecological indicators that can provide information about ecosystem health status and structure.

This paper intends to identify and test several methods and variables applicable to airborne and terrestrial stationary laser scanning to quantify the capacity of the forest ecosystem in providing benefits. The identification of suitable ecosystem services will be performed according to The Economics of Ecosystem and Biodiversity (TEEB) classification [51,55]. Alongside, Millennium Ecosystem Assessment classification (MEA) and Common International Classification of Ecosystem Services (CICES), TEEB represents one of the widely known ecosystem services classification networks. The latter is a global campaign aiming at raising awareness regarding biodiversity's economic benefits and the rising costs of ecosystem degradation. The final purpose of this initiative is to analyze and explain in a mainstream approach the importance of taking action [56]. This classification was adopted because it corresponds faithfully to the functions attributed to the studied stands according to the Romanian forest legislation. The majority of ecosystem functions will be analyzed in relation to the existing indicators, as well as other variables adapted to active remote-sensing sampling. The paper does not intend to calibrate or to validate existing methodologies but to showcase a minimal set of indicators computed through active remote-sensing methods that can offer sufficient information about the ecosystems' capacity to provide services. Furthermore, as mentioned above, the paper aims only at information obtained through the use of ALS and stationary TLS measurements, excluding any other potential data based on satellite imagery or other passive remote-sensing technologies.

2. Materials and Methods

2.1. Study Site

To analyze the identified methods and variables, ten stands were considered in the current study, each of them being designed as a one-hectare rectangular plot with three 15 m-radius circular subplots within them.

The ten one-hectare plots are located in two different areas of the Southern Carpathian mountains, thus covering three of the most representative tree species of Romania. These are sessile oak (*Quercus petraea*) and beech (*Fagus sylvatica*) in the hill region and Norway spruce (*Picea abies*) in the mountainous region (Figure 1).

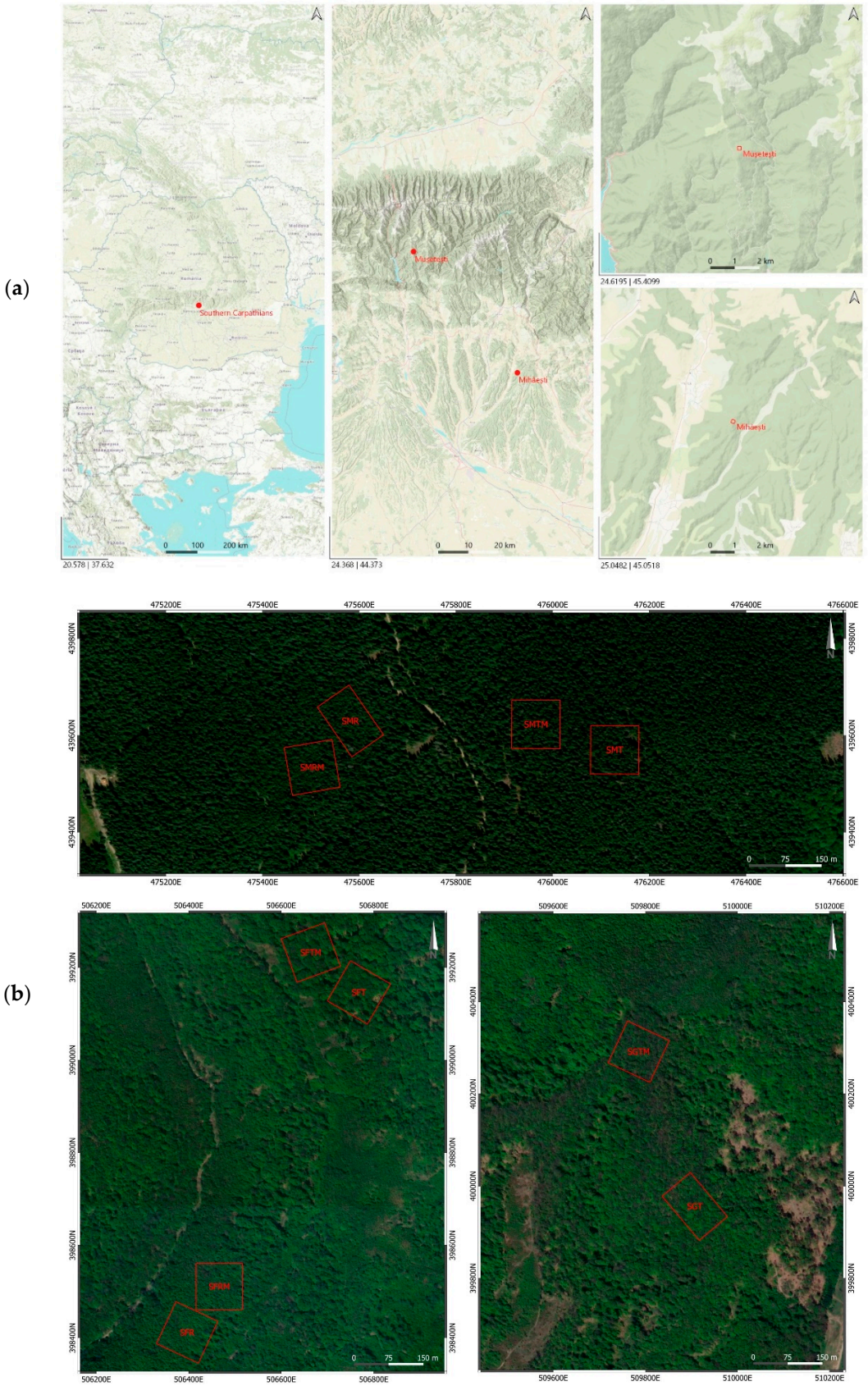

Figure 1. (**a**) Location of the sampled forest stands, (**b**) detailed position (coordinates in WGS 84 projection system).

Both deciduous and coniferous forest plots were considered in the process of assessing the applicability of the studied methods as well as in the evaluation of the different

structural characteristics of the plots. Therefore, the plots were chosen in relation to species, age, and applied silvicultural interventions (Table 1).

Table 1. Sample plots characteristics.

Sample Plot	Species	Age [Years]	Silvicultural Interventions	Forest Districts
SGT	Sessile oak	190	Progressive	Mihăești
SGTM	Sessile oak	190	Without interventions	Mihăești
SFR	Beech	40	Thinning	Mihăești
SFRM	Beech	40	Without interventions	Mihăești
SFT	Beech	120	Progressive	Mihăești
SFTM	Beech	120	Without interventions	Mușetești
SMR	Norway spruce	50	Thinning	Mușetești
SMRM	Norway spruce	50	Without interventions	Mușetești
SMT	Norway spruce	150	Progressive	Mușetești
SMTM	Norway spruce	150	Without interventions	Mușetești

2.2. Conventional Field Data Collection

In order to ensure control over the LiDAR data sets, a classical inventory was also carried out in the plots. Field measurements included DBH, tree height, crown height, crown width, and position of each tree (XYZ coordinates) and targeted all the trees with a DBH equal to or greater than 6 cm. To acquire these variables, an integrated GIS field software and electronic mapping and dendrometrics sensors [57] for recording tree positions and canopy characteristics were used.

2.3. Terrestrial Laser Scanner Data

In each 15 m circular subplot, five terrestrial scans were performed accordingly to a cardinal point sampling scheme to compensate for the shadowing (Figure 2a). The scanning process was achieved with a phase shift terrestrial laser scanner [58]. The resulting point clouds were characterized by 8 µs per scan point and over 44 million points per 360° sweep.

(**a**)

Figure 2. *Cont.*

(**b**)

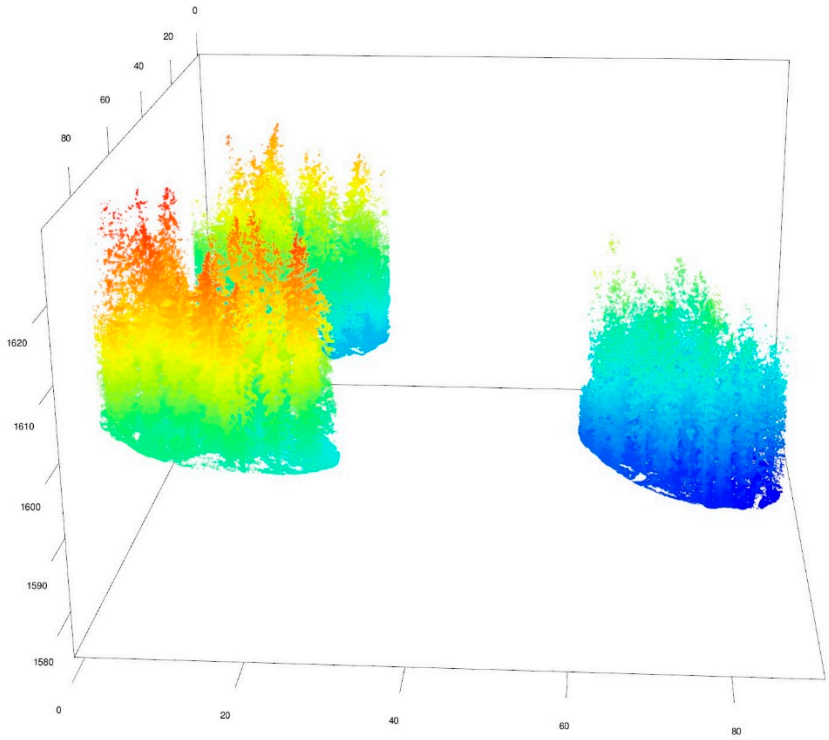

Figure 2. (**a**) TLS ground-based data collection (**b**) terrestrial laser scan of the subplots.

Regarding the TLS pre-processing methods for classification and segmentation of the point cloud prior to obtaining the stems and the foliage, an approach proposed by Pascu et al. was followed [24,30,32,59] (Figure 2b).

2.4. Airborne Laser Scanner Data

The airborne LiDAR data for the one-hectare plots were collected through the use of a full-wave airborne laser scanner [60]. The discrete points extraction was conducted by the provider of the data sets, according to the standard processing procedure. Following processing, an average point density of 6 points/m^2 was reached (Figure 3).

Further analyses, such as the ground-non-ground classification, were performed using filtering algorithms by means of dedicated software [61], as shown in the work of [62]. The digital terrain model (DTM) was generated through an inverse distance-weighting interpolation, which ensured a 1 × 1 m spatial resolution. The DTM was further used as support in the computation of several parameters (e.g., tree height, canopy height).

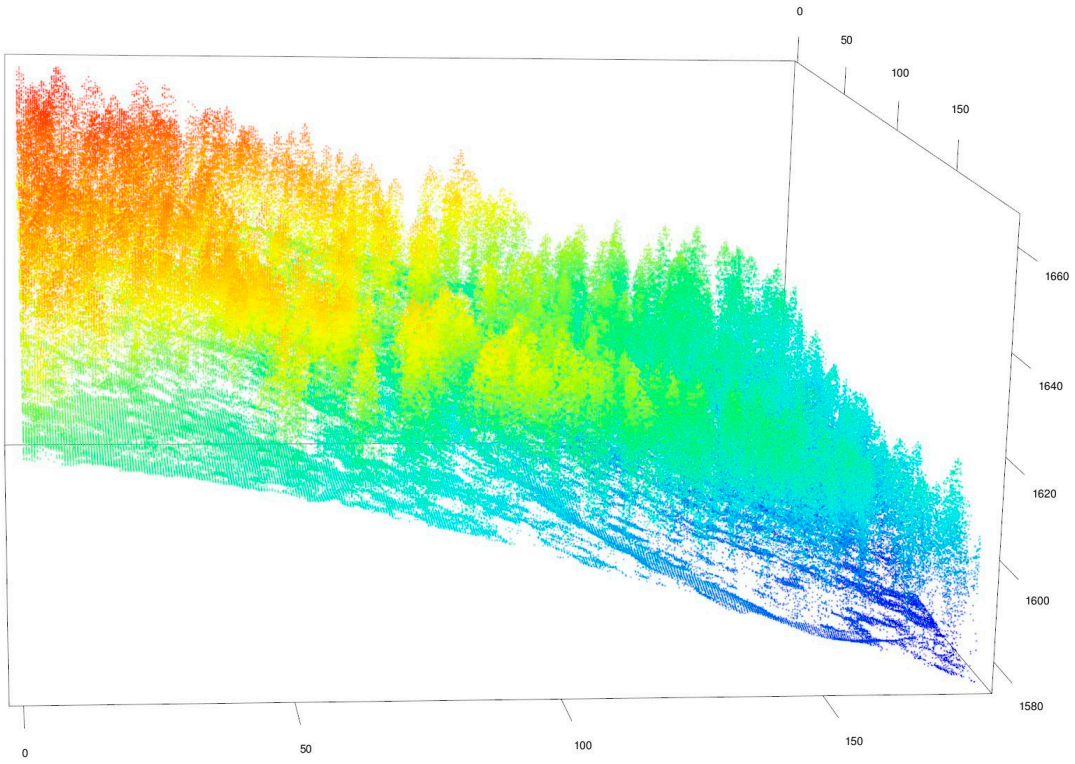

Figure 3. Airborne laser scan of the studied area.

2.5. Ecosystem Services Identification and Evaluation

The literature proposes an entire series of ecosystem functions and services assessment methods (monetary, non-monetary, and integrated methods). In this research, the interest was to gather reliable information needed in applying those evaluation methods. The ecosystem services identification is presented according to the ecosystem functions stated by TEEB, and the paper intends to cover the majority of the functions.

3. Results

3.1. Provisioning Services

Wood products are one of the most prominent resources provided by forest ecosystems [63], being a direct economic benefit that can be easily assessed from a monetary point of view. In literature, wood products, equated to above-ground biomass, are an important variable that can be estimated through remote-sensing techniques. Between the implementation of biophysical parameters relationships [64,65] to allometric models and direct measurements [30,66–68], the above-ground biomass estimation gained impressive interest in research due to the associated accuracy.

In our study, the applied methodology was the one proposed by Pascu et al. in the work of [30]. Therefore, the above-ground estimation implied the use of stand volume derived from number of trees, DBH, and tree height (Figure 4). Even though other studies [69,70] show volume underestimation when based on terrestrial laser scanning data, this was due to low stand heterogeneity. The accuracy presented by Pascu et al. in what concerns the number of trees and DBH is more than satisfactory (errors under 5%). Moreover, the use of terrestrial laser scanning proved to be an adequate approach for the above-ground volume computation [71].

Height values computed through this active remote-sensing technology show biases and errors, also highlighted by several research papers [30,69,70,72,73]. To overcome this limitation, compensations were applied based on airborne laser scanning.

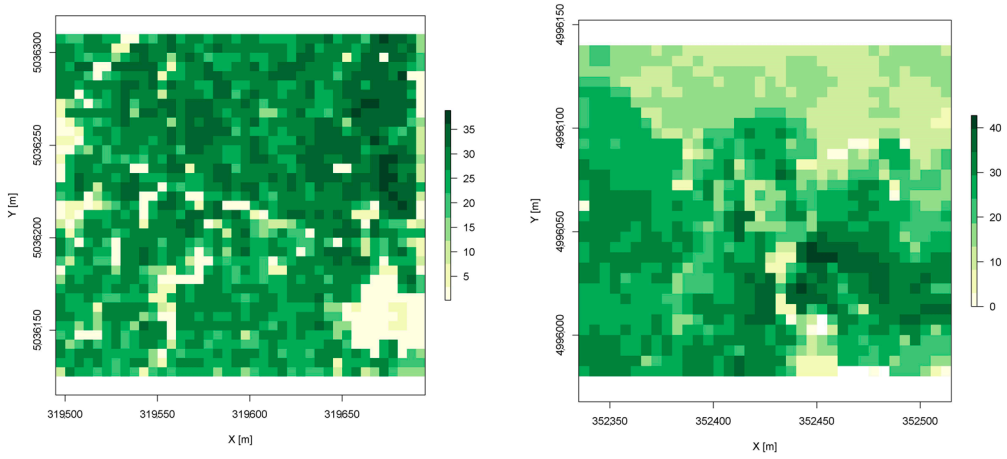

(**a**) (**b**)

Figure 4. Canopy height model from airborne laser scanning (**a**) SMTM (**b**) SGTM.

For computing above-ground tree volume, the logarithmic regression equation (Equation (1)) described in the work of [74] was used:

$$\log v = a_0 + a_1 \log d + a_2 log^2 d + a_3 \log h + a_4 log^2 h \quad (1)$$

where:

d—tree diameter at breast height;
v—tree volume;
h—tree height;
a_0, a_1, a_2, a_3, a_4—species-specific regression coefficients.

The above-ground volumes for each plot are presented in Table 2. When compared to the field measurements based on the same methodology (Equation (1)), the errors are between 4.6% and 13.3%.

Table 2. Above-ground volume and mean stand characteristics.

Plot	V [m^3 ha^{-1}]	d_m [cm]	h_m [m]	v_m [m^3]
SGT	444.1	21.91	20.7	0.97
SGTM	646.4	24.15	22.36	0.90
SFR	434.6	17.81	21.9	0.37
SFRM	509.8	18.25	26.26	0.48
SFT	457.2	24.83	18.9	1.07
SFTM	622.3	25.45	19.4	1.05
SMR	345.7	17.3	17.8	0.28
SMRM	420.1	17.45	15.8	0.29
SMT	409.5	29.29	21.6	0.90
SMTM	558.3	33.01	26.6	0.93

V—stand volume; d_m—stand mean diameter; h_m—stand mean height; v_m—tree mean volume.

Considering the biophysical parameters, differences in mean stand volume can be observed between the plots where silvicultural interventions were applied and those without interventions. The reduced volume, specific to the young forest stands and to those targeted by interventions, confirms the viability of the methods and results and makes it possible to compare them in terms of wood product provisioning.

3.2. Regulating Services

At the moment, the ecosystem services specific to regulating functions represent a great challenge in the evaluating processes [54]. This function includes services for air quality regulation, moderation of extreme events, erosion prevention, and carbon

sequestration [51,55,75]. In the context of evaluating the related services, specific indicators were developed in the field of ecological research.

The assessment methods tend to use indirect measurements and quantify the relationship between different variables. Tree canopy cover, canopy structure indices (e.g., leaf area index), and trees distribution are the most used parameters in the majority of the evaluating approaches [76–78].

3.2.1. Structural Indices

As previously mentioned, forest structure characteristics and biodiversity are the main sources of information for the assessment of ecosystem services. To establish the capacity of ecosystems in supplying regulating services, indices such as Clark-Evans nearest neighbor index (CE), uniform angle index (*UAI*), and relative dominance diameter index were computed at the subplot level.

Clark-Evans nearest neighbor index (CE) describes the horizontal trees distribution by using the mean distance between a reference tree and the nearest neighbors and the mean distance defined by a Poison distribution [79]. CE can range from 0, when the stand is characterized by tree clustering, to 2.1491 [79] in the case of regular distribution.

Uniform angle index (*UAI*) describes the uniform distribution of the nearest neighboring trees in relation to the reference tree [38]. The method is based on the angles between trees, compared to a uniform dispersion angle of 72° (Equation (2)). The interpretation of these values is made according to the confidence interval of 0.475–0.517 [38], describing a random distribution.

$$UAI = \frac{1}{n}\sum_{i=1}^{n} UAI_i = \frac{1}{4n}\sum_{i=1}^{n}\sum_{j=1}^{4} z_{ij} \quad (2)$$

where:

n—number of reference trees

z_{ij}—angle coefficients in relation to the reference (72°), 1 if <72°, 0 if > 72°

UAI_i—uniform angle index

The relative dominance diameter index (IDR) is defined as the ratio between the number of trees with a diameter greater than the reference tree. The value of this indicator reaches values in the range (0–1) and is interpreted in relation to five default thresholds. Thus, in relation to the number of trees with a diameter larger than the reference, the indicator falls into the following categories: shade tolerant, dominated, co-dominant, dominant, predominant. These categories correspond to the Kraft classes, a method used for validating the obtained values. The variable considered in the evaluation of the dominancy indicator may be substituted by other tree characteristics such as height or species.

In the structural indices computation process, the edge effect was removed in order to ensure accurate results. This was performed by selecting only the trees within an inner buffer, defining an area smaller than that of the circular subplots (Figure 5).

The interpretation of these indices made it possible to identify the supplied services and the level to which they could be quantified. CE values greater than 1 suggested that the studied subplots were characterized by a more uniform horizontal structure. An exception was identified in the SFTM-3 subplot, which was characterized by a mean value of 0.4. This could be explained by the smaller number of trees clustered together and by the fact that this circle is crossed by a forest harvesting road. Based on the calculated t-values for the CE, according to the work of [80], the subplots that overpass 1.96 can be described as having a regular distribution (Table 3).

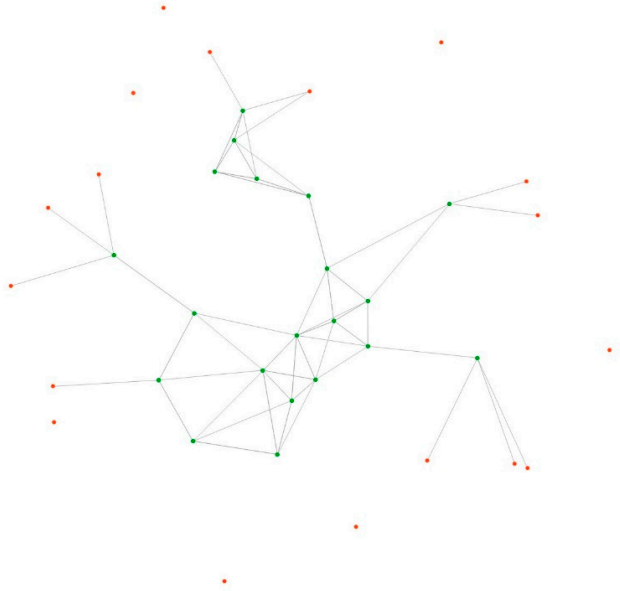

Figure 5. Nearest neighbors identification and reference trees selection; **green**—reference tree; **red**—marginal tree.

Table 3. Horizontal structure indices in the 15 m-radius subplot.

Plots	Subplot	N_{ref}	CE	*t*-Value *	W
SMTM	1	17	1.715	1.19	0.456
	2	11	1.829	2.19	0.432
	3	7	1.689	2.59	0.393
SGTM	1	20	1.558	3.12	0.563
	2	19	1.558	3.14	0.526
	3	25	1.825	2.68	0.510
SFTM	1	31	1.074	0.56	0.547
	2	37	1.272	1.59	0.574
	3	20	0.405	−8.75	0.55
SFRM	1	64	1.423	1.09	0.553
	2	55	1.283	0.91	0.515
	3	37	1.166	0.97	0.5
SMRM	1	92	1.269	0.4	0.532
	2	106	1.171	0.21	0.709
	3	87	1.025	0.04	0.548
SMT	1	46	1.751	3.17	0.531
	2	55	1.604	1.95	0.524
	3	38	1.429	2.41	0.561
SGT	1	39	1.321	2.7	0.545
	2	38	1.556	2.13	0.59
	3	35	1.575	3.65	0.558
SFT	1	26	1.551	4.46	0.635
	2	42	1.781	3.77	0.642
	3	36	1.549	3.34	0.643
SFR	1	71	1.309	0.68	0.715
	2	99	1.866	1.16	0.707
	3	76	1.628	0.95	0.725
SMR	1	102	1.301	0.38	0.719
	2	131	1.244	0.21	0.722
	3	147	1.252	0.37	0.723

N_{ref}—number of reference trees, * *t*—CE value.

When uniform angle index values were analyzed, differences between plots could be observed, thus detecting structural differences between the corresponding stands. The uniform angle index values ranged between 0.393 and 0.725, values covering the entire interpretation interval. Within the old sessile oak stand, without interventions (SGTM), the corresponding subplots reached values equivalent to a rather random distribution. This was the case with the 2.3 (0.510) subplot, reaching values quite different than its counterpart, subplots 2.1 and 2.2, characterized by a clustered structure (Table 2). In the case of the Norway spruce (SMTM), the reached values defined a uniform structure, while the young beech stand with interventions (SFR) was characterized by a clustered structure in all subplots.

Also, from this analysis, the difference between the plots with interventions and those without could be observed. The plots covered with silvicultural treatments tend to describe more clustered structures, an effect caused by the increased distance between trees after harvesting.

Figure 6 facilitates the interpretation of the structure and conditions similarity within a plot. As stated before, discrepancies appeared in SFTM for the CE index and in SMRM for the uniform angle index. The latter was a consequence of a windthrow event that had affected the SMRM-3 subplot.

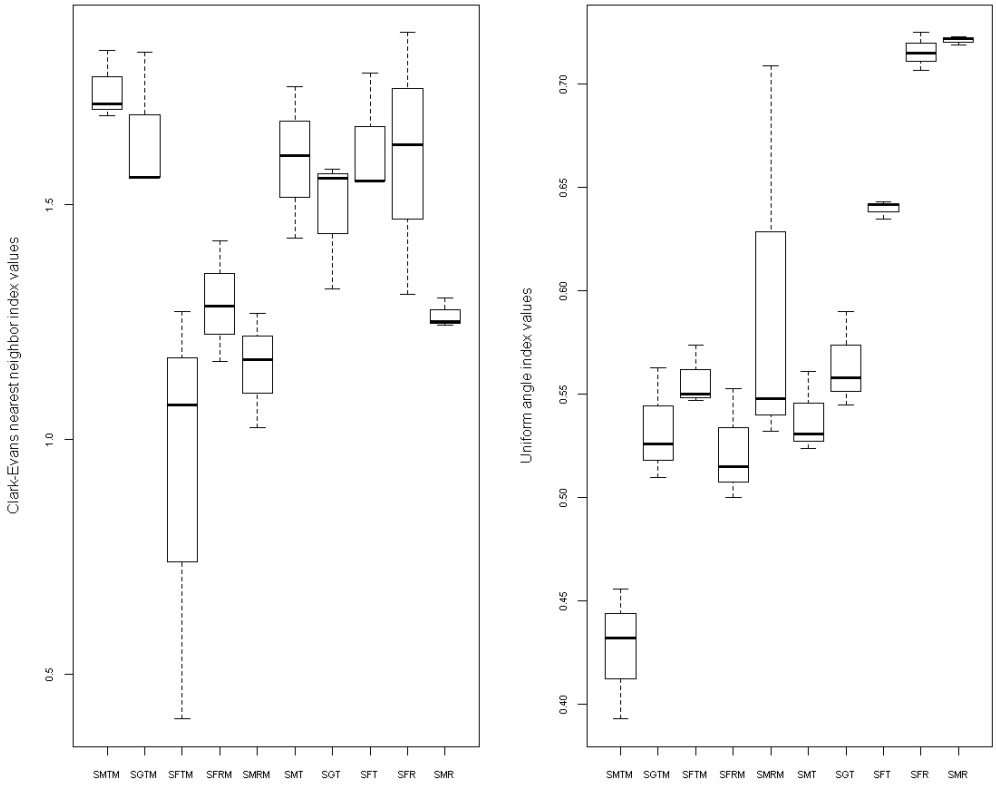

Figure 6. Clark-Evans nearest neighbors index and uniform angle index.

Analyses of relative dominance diameter index described the vertical stand structure at the subplot level. A similarity could be observed between old Norway spruce (SMTM) subplots (Figure 7), indicating a uniform structure within the stand and a uniform tree distribution between classes. The sessile oak stand is characterized by a lower degree of heterogeneity and more unevenness between classes.

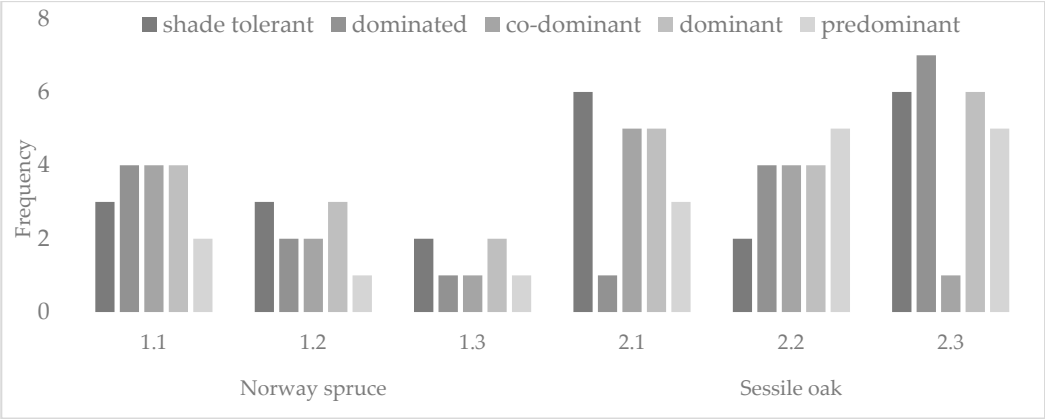

Figure 7. Vertical stand structure (Kraft classes) based on IDR.

3.2.2. Carbon Storage

Carbon is stocked in forest stands in the following five pools: above and below-ground living biomass, soil, litter, and deadwood [81,82]. Apart from the variables used for the above-ground volume, carbon stock evaluation (Table 4) required another set of parameters, namely the theoretical number of trees per hectare, wood density, root-to-shoots ratio, and biomass expansion factor (Equation (3)). These were retrieved from specific yield tables and international guides [83,84].

$$C_{stock} = \sum V * D * (1 + R) * BEF * CF \quad (3)$$

where:

C_{stock}—carbon stock [tC]
V—tree volume [m^3]
D—wood density [t/m^3]
R—root-to-shoot ratio
BEF—biomass expansion factor
CF—carbon fraction

Table 4. Carbon stock required variables.

Plot	V [m^3 ha^{-1}]	D [1] [kg m^{-3}]	R [1]	BEF [2]	CF [3]	Carbon Stock [tC·ha^{-1}]
SGT	444.1	584	0.22	1.4	0.48	151.88
SGTM	646.4	584	0.22	1.4	0.48	221.06
SFR	434.6	545	0.19	1.4	0.46	129.66
SFRM	509.8	545	0.19	1.4	0.46	152.09
SFT	457.2	545	0.19	1.4	0.46	136.40
SFTM	622.3	545	0.19	1.4	0.46	185.65
SMR	345.7	353	0.2	1.3	0.51	74.68
SMRM	420.1	353	0.2	1.3	0.51	90.76
SMT	409.5	353	0.2	1.3	0.51	88.47
SMTM	558.3	353	0.2	1.3	0.51	120.61

[1] [83] [2] [84] [3] [85].

Due to the methodology for the above-ground volume, for the sessile oak and beech species, the biomass expansion factor (BEF) was omitted, as the regression equation for volume already took into consideration the branches' volume. Including BEF would have led to biased results.

The obtained carbon stock values ranged between 74.68 tC·ha^{-1} (273.82 tCO_2·ha^{-1}) in the case of the young Norway spruce plot covered with silvicultural intervention and 221.06 tC·ha^{-1} (810.55 tCO_2·ha^{-1}) in the case of the old sessile oak plot. The upper values

of the storage capacity interval of the studied plots are in accordance with those stated in the work of [86]. The lower values are a consequence of age and species characteristics (wood density, root-to-shoot ratio, and carbon fraction).

3.2.3. Foliage Indices

Active remote-sensing technology advances allowed for the development of multiple applications addressing the canopy structure, crown dynamics, and phenology [21,24,29,87–91]. These applications based on active remote-sensing data are a powerful tool in the decisional process associated with forestry and ecology sectors. From the variety of indices computed through remote sensing, in the research field, the leaf area index (LAI) is the most commonly used. Furthermore, along with the LAI, an important role in improving the canopy description is held by leaf area density (*LAD*), which offers detailed information regarding the stand vertical structure. Leaf area index estimation as the ratio between leaves (single-faced) area and area of the studied plot, was measured over time through various indirect methods (orbital sensors, hemispherical photography, and light intensity attenuation) [92–94], and still require improvement in what concerns the stability and robustness of their results. Alternatively, airborne laser scanning, despite its limitations related to penetration capability, has promising results in forestry indices and parameters computation, including those above-mentioned [70,95].

In this study, LAI and *LAD* were estimated through the MacArthur and Horn equation [96] developed on the principle of the Beer–Lambert law [97,98] and following methodologies proposed in other related research papers [95,99–102]. Thus, to each voxel from the processed point cloud (voxel—5 × 5 × 1 m), the following proposed equation was applied [102]:

$$LAD_{i-1,i} = \ln\left(\frac{S_e}{S_t}\right)\frac{1}{k\Delta z} \quad (4)$$

where:

S_e—number of pulses entering the voxel;
S_t—number of pulses exiting the voxel;
k—Beer–Lambert law extinction coefficient;
z—voxel height (1 m).

From the variety of estimated indices resulting when applying derivatives of the above-mentioned methodology, of most interest to our study were the total LAI values, the height of the mean *LAD*, and standard deviation corresponding to each voxel (cell of a three-dimensional grid) column taken into consideration.

As shown in the case of the IDR, sessile oak (SGTM) is characterized by an uneven structure, a fact also illustrated in the LAI and *LAD* values. In the northwest part of the plot, the higher density of smaller trees impacted the LAI and height of the mean *LAD*, reaching values in the range 1–3, respectively, 5–10 m.

As expected, the Norway spruce plot is characterized by smaller standard deviation values, suggesting a constant horizontal structure throughout the plot (Figure 8). In the case of the sessile oak plot, the standard deviation trend highlights a generation individualization through higher variation within the upper levels of the canopy.

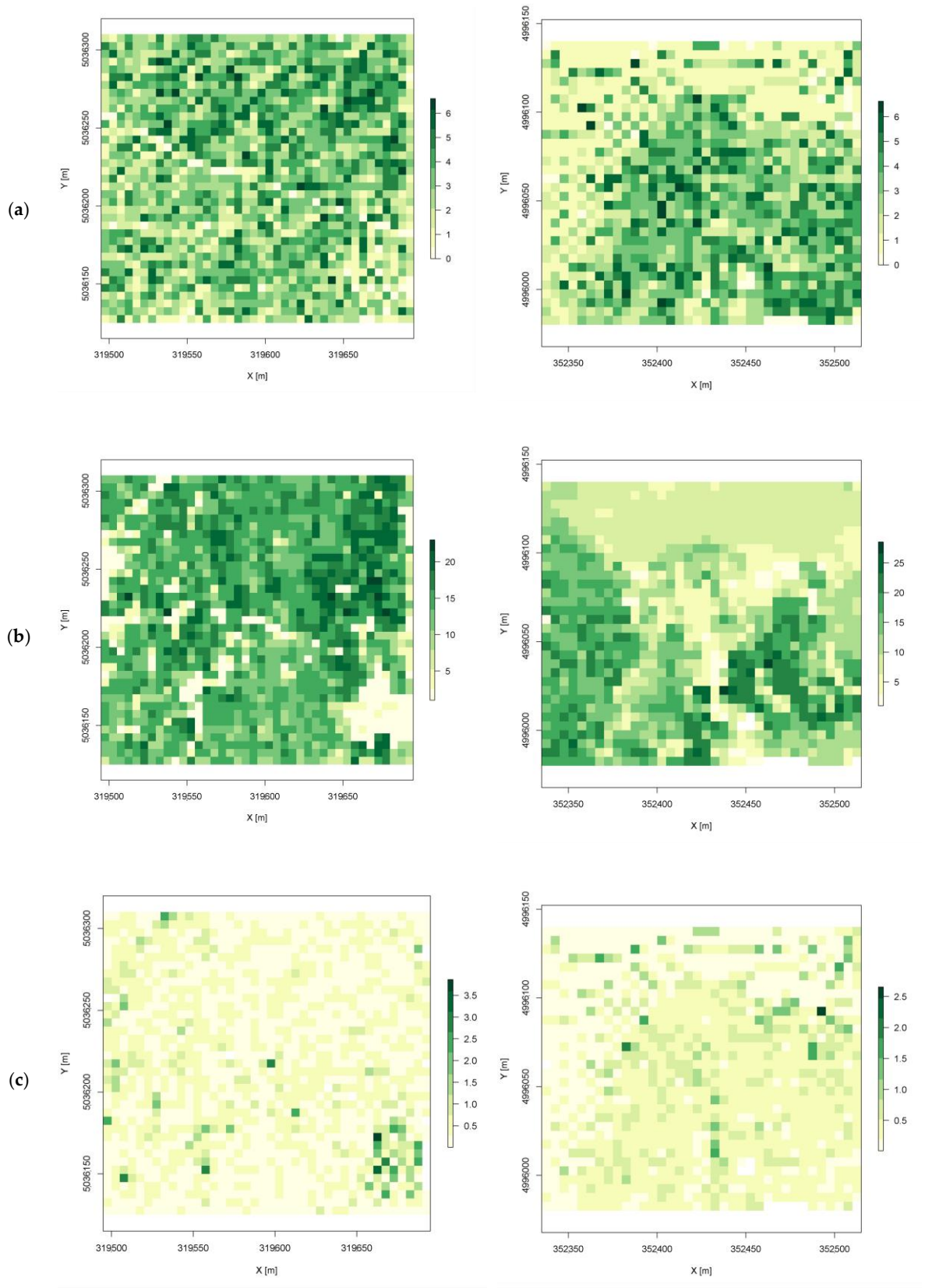

Figure 8. Mapped values of (**a**) LAI; (**b**) height of the mean *LAD*; (**c**) standard deviation corresponding to each voxel column.

3.3. Supporting Services

In the majority of the research papers, this function is not a self-contained one. Millennium Ecosystem Assessment classification (MEA) [103] presents the support function as integration between provisioning, regulating, and cultural functions, quantifying benefits that ensure the rest of the services. In the Common International Classification of Ecosystem Services (CICES), the support function is not promoted as one and is considered an underlying structure that provides indirect outputs [104,105].

Understory biomass has an important ecological significance in forest ecosystem stability and in assessing the relationships between wildlife and their habitat. Despite the low proportion in above-ground volume, the understory biomass represents a tool for the researchers in evaluating the food provisioning and the quality of the environment [106–114].

The understory biomass computation implies a complex and expensive forest inventory due to multiple variables that should be taken into consideration. Active remote-sensing applications that aim at assessing understory biomass were proposed. Terrestrial and airborne laser scanning data were analyzed in order to estimate the understory, following [106,112,115].

This study addressed the methodology proposed by the authors of [116] that aims to predict the presence of shrub layers from aerial-based point clouds. In the mentioned thesis, two indices were computed: (a) undergrowth return fraction and (b) undergrowth cover density. For our case, of most interest was the undergrowth return fraction, expressed as the ratio between the number of points in the 0.5–5 m range and the total number of points (Figure 9).

The old Norway spruce plot, in comparison with the sessile oak, is characterized by a sparse distribution of the shrub layer of lower intensities, with no understory clusters identified. In the case of the sessile oak plot, a central area with a high density of understory vegetation could be observed, mirrored in the northern part, by the lower values of the canopy height model. Overall, the sessile oak plot recorded a value of 0.20, which according to the work of [116], is indicative of a medium-to-high shrub cover intensity (Figure 10).

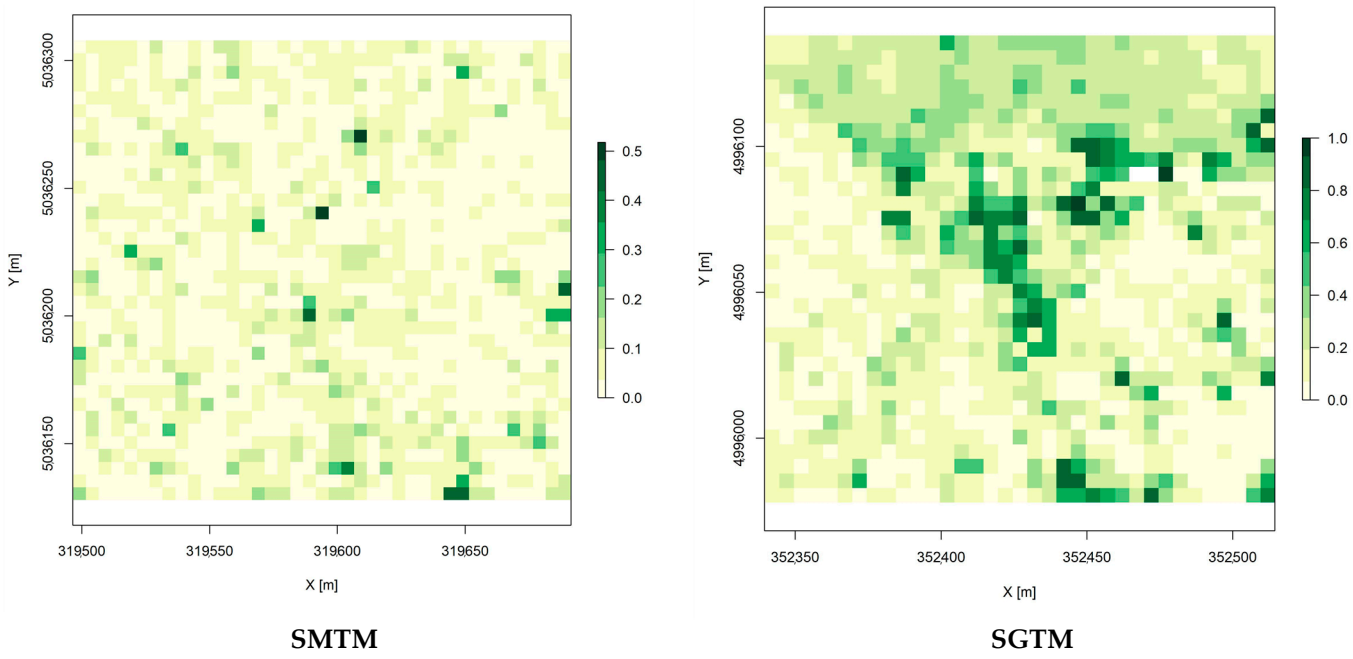

Figure 9. Mapping of the shrub layer (5 × 5 m pixel)—undergrowth return fraction.

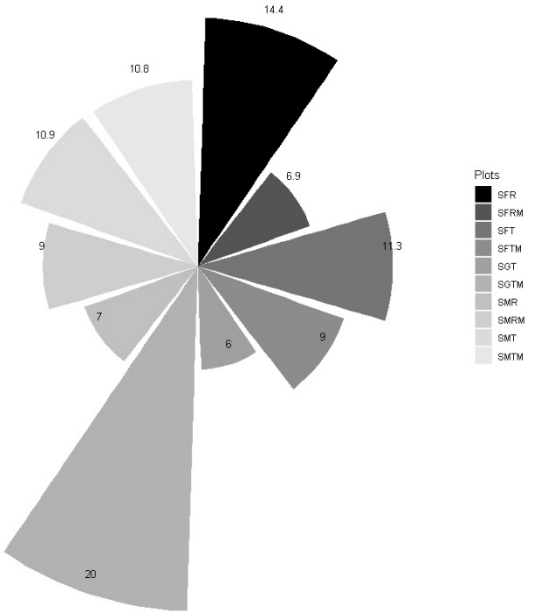

Figure 10. Undergrowth return fraction values.

The majority of the rest of the plots have a low-to-minim shrub cover, covering 6% to 10%. An issue identified through field observations was in the case of SMRM. The plot is characterized by a high shrub coverage, but due to the lower age and high tree density, the laser beams could not penetrate the canopy layer. This resulted in a small number of points near the ground and an underestimation of the shrub layer. This shortcoming can be compensated by using TLS data to complete the ALS points cloud.

3.4. Structure Analysis for Cultural Services Assessment

The cultural services are the most problematic in what concerns the evaluation processes. The services provided by the one-hectare plots are not traded on the market, and therefore the methods of valuation applied tend to be more subjective. In addition, the evaluation of the forest ecosystem's capacity in providing these benefits is a challenging one due to public preferences and the number of variables involved.

The forest structure indices computed under the regulating function section and part of the health status information can be used in quantifying the human preferences regarding the ideal distribution and biodiversity. Tree clusters, number of trees, sparse distribution, higher canopy density, light penetration, visibility, understory volume, and snags volume can all be indirectly assessed through tree distribution characteristics and mortality analysis.

The snags identification and mortality characteristics were analyzed based on airborne laser scanning data according to the work of [117] methodology (Figure 11).

After processing, the point clouds were classified into four classes, namely live trees, small snags, live crown edge snags, and higher canopy snags. Due to the small proportion of dead trees in the studied plots, not all classes were well represented. Moreover, following the analysis, none of the snag classes were identified in the Norway spruce plots, apart from sparse, unrepresentative small snags in the understory. By way of comparison, the sessile oak plot presents a higher proportion corresponding to the live crown edge snags class.

A crucial role is attributed to the higher canopy snags class, which makes possible the identification of dead treetops. A higher proportion of snags would have allowed for the evaluation of a ratio between deadwood and the above-ground biomass. This information could have then been used in the carbon sequestration estimation or the mortality rate of the forest stand.

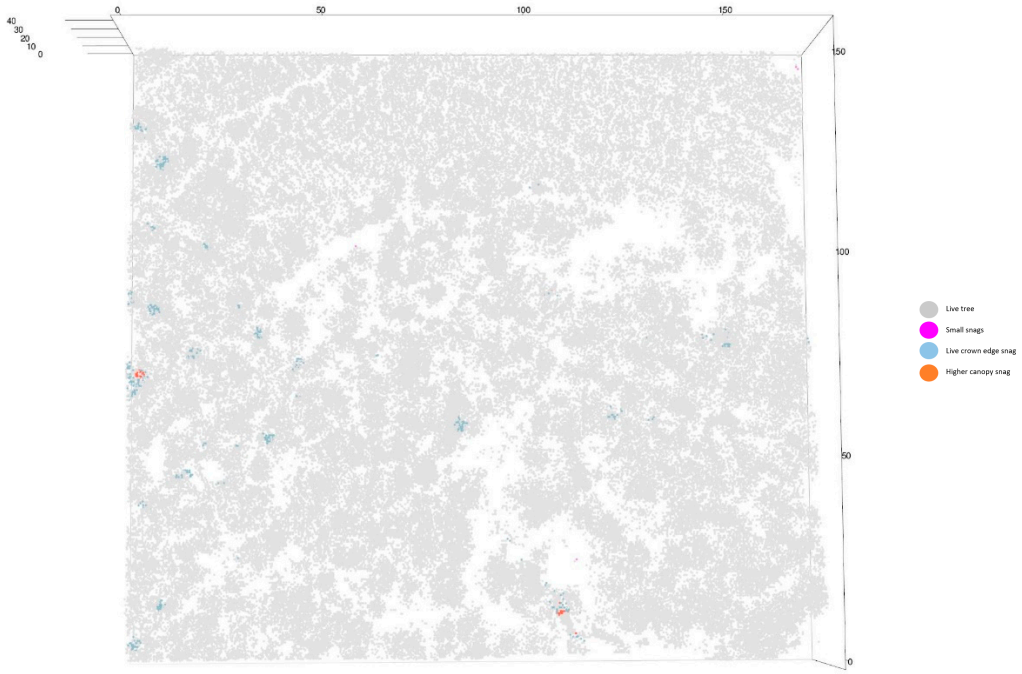

Figure 11. Snags identification and classification (SGTM).

4. Discussion

Forest ecosystems are characterized by various structures and complex processes defined by a plethora of intra- and inter-plot relationships. The assessment of all services provided by these ecosystems' characteristics is still a challenging subject for the research field [118]. Therefore, this study aimed to highlight some of the most important and quantifiable services employing the latest applications of active remote-sensing technology [119].

Taking advantage of the terrestrial stationary laser scanning, the obtained values for above-ground volume, at tree and stand level, was within the characteristic tolerances [30]. Moreover, we compensated the height-specific bias caused by the terrestrial laser scanner's inability to penetrate dense canopies, a well know feature relevant to Romanian forests [24], by deriving a canopy height model from aerial laser scanning.

Compared to the rest of the functions, provisioning could be evaluated most straightforward [76,120]. By only knowing the above-ground volume and market price, this service could be monetized. To better understand this service, a technical approach can further be used by classifying the wood in relation to the type of final product or the quality of the timber, information that can be extracted from management plans.

The assessment of carbon sequestration is a more complex process, and it partially uses wood volume calculations. The results are influenced by multiple biophysical parameters (wood density, the ratio between above and below-ground biomass, or the biomass expansion factor) [84]. All these parameters depend on the species composition, a feature that cannot be presently assessed on a large scale by means of close-range active remote sensing [121,122]. Furthermore, as described in the IPCC Guideline [84,123], forest ecosystems stock a large amount of carbon not only in living biomass, so other pools (soil and dead organic matter) should also be taken into consideration for a real carbon emission/removals analysis. On the other hand, assumptions are made even within the country-level estimation. Pools as soil, deadwood, or litter are considered to be neutral in the carbon emission and removals balance. Therefore, only considering the living biomass can represent a viable solution for carbon sequestration and stock assessment.

The utility of structural indices was highlighted in a long list of studies [24,119,124–126], and the indirect quantification made by means of these indices could be considered a proper method for evaluating forest ecosystem capacity to provide services. Forest structure

represents a valuable source of information, and relating structure characteristics to specific services is the approach used in this study.

Soil and water regulation services assured by the forest ecosystem are quantifiable through trees distribution, LAI, *LAD*, and canopy projection [127,128]. The distances, the angles, and the relationship between different individuals define the rate of success of the forest to ensure the regulation function. Indices such as uniform angle index, Clark-Evans nearest neighbor index, and relative dominance diameter index can describe the ideal structure, which prevents gaps or corridors from occurring. The resulting values, corresponding to the studied plots, describe a uniform tree distribution. According to the uniform angle index values, the Norway spruce plot has a better capacity to assure the regulation function if we consider the ideal structure being a random one.

When analyzing the CE, the obtained values tend to reach the upper half of the range, close to a perfectly regular hexagonal distribution (2.1491). There are some dissimilarities between CE and *UAI* regarding, in particular, the sessile oak plot due to the high number of trees in the sampled area. However, of great importance in soil and water regulation services is the fact that none of the plots is characterized by clustered trees that would facilitate soil erosion and low water retention.

Air regulation function was evaluated in this study through the use of LAI and *LAD* [129]. The capacity of the forest ecosystem to provide these services is directly proportional to LAI values. For the studied plots, LAI values are within the 0–6 range, with a considerable proportion in the upper classes throughout the entire old Norway spruce plot. Due to lower values in the canopy height model and implicit smaller crown volumes, the sessile oak recorded lower intensities in the northern part of the plot.

The support function assessment was evaluated based on the shrub cover, indicating the capacity of the studied forests to provide various species' habitat requirements. Important differences were observed between the studied areas. The sessile oak plot (SGTM) recorded a larger area covered by understory vegetation. This analysis can also provide additional information on the forest structure, information that can be used in further biodiversity assessments.

The results regarding mortality have not allowed any further analyses regarding the dead matter stratification. However, it offered enough information to assess the overall health status of the forest ecosystem [117,123,130]. By following the presented structural indices, as well as the ones addressing foliage, while simultaneously considering the human preferences toward the ideal forest structure, a suitable evaluation of the cultural services could be deployed.

Given the results corresponding to our studied plots, the lack of clustered trees, large gaps, and overall canopy structure, an appropriate scale for referencing forest ecosystems' capability to provide cultural benefits could have also been developed.

5. Conclusions

In order to emphasize and maximize the ecological, social, and economic benefits of forests, suitable assessment methods are required. Active remote-sensing technology, with the proven advantages and characteristic limitations, can represent the foundation for multiple approaches aiming to quantify the capacity of the forest ecosystem to provide services. This study highlighted the possibility of using two different active remote-sensing data sets and several techniques to assess the main ecosystem functions according to TEEB classification.

To estimate the key biophysical parameters of a tree, terrestrial laser scanning point clouds proved to be a viable solution. The processing of this data source led to errors associated with DBH of below 1 cm [30] at the subplot level when analyzing the mean tree. Precisions associated with tree coordinates are comparable to those obtained through the electronic field mapping system. Using the TLS-based variables as well as the airborne laser scanning data, the provisioning function, particularly wood products, was evaluated.

This was performed by means of above-ground volume, characterized by errors smaller than 6%.

Combining the terrestrial and aerial laser scans, the evaluation of regulating function was also possible. The indices computed by processing the above-mentioned data sources proved to be a suitable basis for acquiring the forest's horizontal structure and the distribution of trees. CE, *UAI*, and IDR implementations through active remote-sensing approaches can represent the link between ecosystem services and human preferences, but also the qualitative parameters for assessing the degree of ensuring certain services, namely soil stability, air quality, and water regulation.

Challenges still exist in applying active remote-sensing techniques due to the complex ecosystems' intra- and inter-plot relationships. However, the development of tools to address the environmental assessment requirements is encouraged by the stakeholders and decisional factors. Thus, it can be stated that active remote-sensing applications have a significant role in forestry, a role that translates to an overall improvement of human well-being.

Therefore, implementing the described methodologies highlighted the necessity of developing custom reference scales relevant in the assessment processes of the relative capacity of forest ecosystems to supply benefits. To achieve this, the study should be extended to address further stands of different structures, species compositions, and microclimates.

Author Contributions: Conceptualization, A.C.D., I.-S.P., G.M.T. and O.B.; Formal analysis, A.C.D. and I.-S.P.; Investigation, A.C.D., I.-S.P., Ș.L. and J.G.-D.; Methodology, A.C.D. and I.-S.P.; Software, I.-S.P.; Validation, Ș.L., C.-E.D., G.M.T. and O.B.; Visualization, I.-S.P.; Writing—original draft, A.C.D. and I.-S.P.; Writing—review and editing, A.C.D., J.G.-D., G.M.T., I.-S.P. and O.B. All authors have read and agreed to the published version of the manuscript.

Funding: This study was conducted under the project CRESFORLIFE (SMIS 105506), subsidiary contract no. 18/2020, co-financed by the European Regional Development Fund through the 2014–2020 Competitiveness Operational Program.

Conflicts of Interest: The authors declare no conflict of interest.

References

1. Sasaki, N.; Asner, G.; Knorr, W.; Durst, P.; Priyadi, H.; Putz, F. Approaches to classifying and restoring degraded tropical forests for the anticipated REDD+ climate change mitigation mechanism. *iForest Biogeosci. For.* **2011**, *4*, 1–6. [CrossRef]
2. Pan, Y.; Birdsey, R.A.; Fang, J.; Houghton, R.; Kauppi, P.E.; Kurz, W.A.; Phillips, O.L.; Shvidenko, A.; Lewis, S.L.; Canadell, J.G.; et al. A large and persistent carbon sink in the World's forests. *Science* **2011**, *333*, 988–993. [CrossRef]
3. Fu, X.; Zhang, Z.; Cao, L.; Coops, N.C.; Goodbody, T.R.; Liu, H.; Shen, X.; Wu, X. Assessment of approaches for monitoring forest structure dynamics using bi-temporal digital aerial photogrammetry point clouds. *Remote Sens. Environ.* **2021**, *255*, 112300. [CrossRef]
4. Badea, O.; Neagu, S.; Bytnerowicz, A.; Silaghi, D.; Barbu, I.; Iacoban, C.; Popescu, F.; Andrei, M.; Preda, E.; Iacob, C.; et al. Long-term monitoring of air pollution effects on selected forest ecosystems in the Bucegi-Piatra Craiului and Retezat Mountains, southern Carpathians (Romania). *iForest Biogeosci For.* **2011**, *4*, 49–60. [CrossRef]
5. Lausch, A.; Borg, E.; Bumberger, J.; Dietrich, P.; Heurich, M.; Huth, A.; Jung, A.; Klenke, R.; Knapp, S.; Mollenhauer, H.; et al. Understanding forest health with remote sensing, part III: Requirements for a scalable multi-source forest health monitoring network based on data science approaches. *Remote Sens.* **2018**, *10*, 1120. [CrossRef]
6. Rasmussen, L.V.; Jepsen, M.R. Monitoring systems to improve forest conditions. *Curr. Opin. Environ. Sustain.* **2018**, *32*, 29–37. [CrossRef]
7. Grafström, A.; Zhao, X.; Nylander, M.; Petersson, H. A new sampling strategy for forest inventories applied to the temporary clusters of the Swedish national forest inventory. *Can. J. For. Res.* **2017**, *47*, 1161–1167. [CrossRef]
8. Ginzler, C.; Hobi, M.L. Countrywide stereo-image matching for updating digital surface models in the framework of the swiss national forest inventory. *Remote Sens.* **2015**, *7*, 4343–4370. [CrossRef]
9. Masek, J.G.; Hayes, D.; Hughes, M.J.; Healey, S.P.; Turner, D.P. The role of remote sensing in process-scaling studies of managed forest ecosystems. *For. Ecol. Manag.* **2015**, *355*, 109–123. [CrossRef]
10. Lechner, A.M.; Foody, G.M.; Boyd, D.S. Applications in remote sensing to forest ecology and management. *One Earth* **2020**, *2*, 405–412. [CrossRef]

11. Boyd, D.; Foody, G. An overview of recent remote sensing and GIS based research in ecological informatics. *Ecol. Inform.* **2011**, *6*, 25–36. [CrossRef]
12. Antonarakis, A.; Richards, K.; Brasington, J. Object-based land cover classification using airborne LiDAR. *Remote Sens. Environ.* **2008**, *112*, 2988–2998. [CrossRef]
13. Yan, W.Y.; Shaker, A.; El-Ashmawy, N. Urban land cover classification using airborne LiDAR data: A review. *Remote Sens. Environ.* **2015**, *158*, 295–310. [CrossRef]
14. García, M.; Riaño, D.; Chuvieco, E.; Danson, F. Estimating biomass carbon stocks for a Mediterranean forest in central Spain using LiDAR height and intensity data. *Remote Sens. Environ.* **2010**, *114*, 816–830. [CrossRef]
15. Popescu, S.C. Estimating biomass of individual pine trees using airborne lidar. *Biomass Bioenergy* **2007**, *31*, 646–655. [CrossRef]
16. Næsset, E. Estimating tree height and tree crown properties using airborne scanning laser in a boreal nature reserve. *Remote Sens. Environ.* **2002**, *79*, 105–115. [CrossRef]
17. Lim, K.S.; Treitz, P.M. Estimation of above ground forest biomass from airborne discrete return laser scanner data using canopy-based quantile estimators. *Scand. J. For. Res.* **2004**, *19*, 558–570. [CrossRef]
18. Chuvieco, E.; Congalton, R.G. Application of remote sensing and geographic information systems to forest fire hazard mapping. *Remote Sens. Environ.* **1989**, *29*, 147–159. [CrossRef]
19. Chuvieco, E.; Kasischke, E.S. Remote sensing information for fire management and fire effects assessment. *J. Geophys. Res. Space Phys.* **2007**, *112*. [CrossRef]
20. Jaboyedoff, M.; Oppikofer, T.; Abellan, A.; Derron, M.-H.; Loye, A.; Metzger, R.; Pedrazzini, A. Use of LIDAR in landslide investigations: A review. *Nat. Hazards* **2010**, *61*, 5–28. [CrossRef]
21. Lim, K.; Treitz, P.; Wulder, M.; St-Onge, B.; Flood, M. LiDAR remote sensing of forest structure. *Prog. Phys. Geogr. Earth Environ.* **2003**, *27*, 88–106. [CrossRef]
22. Jayathunga, S.; Owari, T.; Tsuyuki, S. Evaluating the performance of photogrammetric products using fixed-wing UAV imagery over a mixed conifer-broadleaf forest: Comparison with airborne laser scanning. *Remote Sens.* **2018**, *10*, 187. [CrossRef]
23. Palace, M.W.; Sullivan, F.B.; Ducey, M.J.; Treuhaft, R.N.; Herrick, C.; Shimbo, J.Z.; Mota-E-Silva, J. Estimating forest structure in a tropical forest using field measurements, a synthetic model and discrete return lidar data. *Remote Sens. Environ.* **2015**, *161*, 1–11. [CrossRef]
24. Pascu, I.-S.; Dobre, A.-C.; Badea, O.; Tănase, M.A. Estimating forest stand structure attributes from terrestrial laser scans. *Sci. Total. Environ.* **2019**, *691*, 205–215. [CrossRef] [PubMed]
25. Wulder, M.; Hall, R.J.; Coops, N.; Franklin, S. High spatial resolution remotely sensed data for ecosystem characterization. *BioScience* **2004**, *54*, 511–521. [CrossRef]
26. Lefsky, M.A.; Cohen, W.B.; Parker, G.G.; Harding, D.J. Lidar remote sensing for ecosystem studies. *Bioscience* **2002**, *52*, 19–30. [CrossRef]
27. Holmgren, J.; Nilsson, M.; Olsson, H. Estimation of tree height and stem volume on plots using airborne laser scanning. *For. Sci.* **2003**, *49*, 419–428.
28. McRoberts, R.E.; Tomppo, E.O. Remote sensing support for national forest inventories. *Remote Sens. Environ.* **2007**, *110*, 412–419. [CrossRef]
29. Lefsky, M.; Cohen, W.; Acker, S.; Parker, G.; Spies, T.; Harding, D. Lidar remote sensing of the canopy structure and biophysical properties of Douglas-Fir Western Hemlock Forests. *Remote Sens. Environ.* **1999**, *70*, 339–361. [CrossRef]
30. Pascu, I.-S.; Dobre, A.-C.; Badea, O.; Tanase, M.A. Retrieval of forest structural parameters from terrestrial laser scanning: A Romanian case study. *Forests* **2020**, *11*, 392. [CrossRef]
31. Cabo, C.; Ordóñez, C.; López-Sánchez, C.A.; Armesto, J. Automatic dendrometry: Tree detection, tree height and diameter estimation using terrestrial laser scanning. *Int. J. Appl. Earth Obs. Geoinf.* **2018**, *69*, 164–174. [CrossRef]
32. Othmani, A.; Voon, L.F.L.Y.; Stolz, C.; Piboule, A. Single tree species classification from Terrestrial Laser Scanning data for forest inventory. *Pattern Recognit. Lett.* **2013**, *34*, 2144–2150. [CrossRef]
33. Wallace, L.; Lucieer, A.; Malenovský, Z.; Turner, D.; Vopěnka, P. Assessment of forest structure using two UAV techniques: A comparison of airborne laser scanning and structure from motion (SfM) point clouds. *Forests* **2016**, *7*, 62. [CrossRef]
34. Jarron, L.R.; Coops, N.C.; MacKenzie, W.H.; Tompalski, P.; Dykstra, P. Detection of sub-canopy forest structure using airborne LiDAR. *Remote Sens. Environ.* **2020**, *244*, 111770. [CrossRef]
35. Zheng, G.; Moskal, L.M. Retrieving Leaf Area Index (LAI) using remote sensing: Theories, methods and sensors. *Sensors* **2009**, *9*, 2719–2745. [CrossRef] [PubMed]
36. Hosoi, F.; Omasa, K. Voxel-based 3-D modeling of individual trees for estimating leaf area density using high-resolution portable scanning lidar. *IEEE Trans. Geosci. Remote Sens.* **2006**, *44*, 3610–3618. [CrossRef]
37. Zhang, G.; Hui, G.; Zhao, Z.; Hu, Y.; Wang, H.; Liu, W.; Zang, R. Composition of basal area in natural forests based on the uniform angle index. *Ecol. Inform.* **2018**, *45*, 1–8. [CrossRef]
38. Zhao, Z.; Hui, G.; Hu, Y.; Wang, H.; Zhang, G.; Von Gadow, K. Testing the significance of different tree spatial distribution patterns based on the uniform angle index. *Can. J. For. Res.* **2014**, *44*, 1419–1425. [CrossRef]
39. Lausch, A.; Erasmi, S.; King, D.J.; Magdon, P.; Heurich, M. Understanding forest health with remote sensing, Part I: A review of spectral traits, processes and remote-sensing characteristics. *Remote Sens.* **2016**, *8*, 1029. [CrossRef]

40. Listopad, C.M.; Masters, R.E.; Drake, J.; Weishampel, J.; Branquinho, C. Structural diversity indices based on airborne LiDAR as ecological indicators for managing highly dynamic landscapes. *Ecol. Indic.* **2015**, *57*, 268–279. [CrossRef]
41. Wang, K.; Franklin, S.E.; Guo, X.; Cattet, M. Remote sensing of ecology, biodiversity and conservation: A review from the perspective of remote sensing specialists. *Sensors* **2010**, *10*, 9647–9667. [CrossRef] [PubMed]
42. Kerr, J.T.; Ostrovsky, M. From space to species: Ecological applications for remote sensing. *Trends Ecol. Evol.* **2003**, *18*, 299–305. [CrossRef]
43. Duncanson, L.; Niemann, K.; Wulder, M. Estimating forest canopy height and terrain relief from GLAS waveform metrics. *Remote Sens. Environ.* **2010**, *114*, 138–154. [CrossRef]
44. Lefsky, M.A.; Cohen, W.B.; Acker, S.A.; Spies, T.A.; Parker, G.G.; Harding, D. Lidar remote sensing of forest canopy structure and related biophysical parameters at H.J. Andrews experimental forest, Oregon, USA. In Proceedings of the International Geoscience and Remote Sensing Symposium (IGARSS), Seattle, WA, USA, 6–10 July 1998.
45. Daily, G.C.; Matson, P.A. Ecosystem services: From theory to implementation. *Proc. Natl. Acad. Sci. USA* **2008**, *105*, 9455–9456. [CrossRef] [PubMed]
46. Gómez-Baggethun, E.; de Groot, R. Natural capital and ecosystem services: The ecological foundation of human society. *Ecosyst. Serv.* **2010**, *30*, 105–121. [CrossRef]
47. Wyatt, T.D.; de Groot, R.S. Valuing nature. *Glob. Ecol. Biogeogr. Lett.* **1993**, *3*, 90. [CrossRef]
48. Costanza, R.; D'Arge, R.; De Groot, R.; Farber, S.; Grasso, M.; Hannon, B.; Limburg, K.; Naeem, S.; O'Neill, R.V.; Paruelo, J.; et al. The value of the world's ecosystem services and natural capital. *Nature* **1997**, *387*, 253–260. [CrossRef]
49. Balmford, A.; Bruner, A.; Cooper, P.; Costanza, R.; Farber, S.; Green, R.E.; Jenkins, M.; Jefferiss, P.; Jessamy, V.; Madden, J.; et al. Ecology: Economic reasons for conserving wild nature. *Science* **2002**, *297*, 950–953. [CrossRef]
50. De Groot, R.; Brander, L.; van der Ploeg, S.; Costanza, R.; Bernard, F.; Braat, L.; Christie, M.; Crossman, N.; Ghermandi, A.; Hein, L.; et al. Global estimates of the value of ecosystems and their services in monetary units. *Ecosyst. Serv.* **2012**, *1*, 50–61. [CrossRef]
51. Kumar, P. *The Economics of Ecosystems and Biodiversity: Ecological and Economic Foundations*; Earthscan Publications Ltd.: London, UK, 2013.
52. Häyhä, T.; Franzese, P.P. Ecosystem services assessment: A review under an ecological-economic and systems perspective. *Ecol. Model.* **2014**, *289*, 124–132. [CrossRef]
53. Bradbeer, J.; Pearce, D. Economic values and the natural world. *Geogr. J.* **1995**, *161*, 335. [CrossRef]
54. Kornatowska, B.; Sienkiewicz, J. Forest ecosystem services-assessment methods. *Folia For. Pol. A For.* **2018**, *60*, 248–260. [CrossRef]
55. Wittmer, H.; Gundimeda, H. *The Economics of Ecosystems and Biodiversity for Local and Regional Policy Makers*; Routledge: Abingdon-on-Thames, UK, 2011.
56. Sukhdev, P. *The Economics of Ecosystem and Biodiversity*; Yale School of Forestry and Environmental Studies: New Heaven, CT, USA, 2011.
57. IFER. Monitoring and Mapping Solutions. Ltd. FieldMap. 2016. Available online: https://www.youtube.com/watch?v=edBBWh0JyIU&ab_channel=YaleCampus (accessed on 1 March 2021).
58. FARO Technologies Inc. *Faro Scene*; FARO: Lake Mary, FL, USA, 2018.
59. Hackenberg, J.; Spiecker, H.; Calders, K.; Disney, M.; Raumonen, P. SimpleTree—An efficient open source tool to build tree models from TLS clouds. *Forests* **2015**, *6*, 4245–4294. [CrossRef]
60. RIEGL. *LMS-Q680i*; RIEGL Laser Measurement Systems GmbH: Horn, Austria, 2012.
61. Terrasolid Ltd. *TerraScan*; Terrasolid v021 Ltd.: Helsinki, Finland, 2021.
62. Axelsson, P. DEM generation from laser scanner data using adaptive TIN models. *Int. Arch. Photogramm. Remote Sens.* **2000**, *33*, 110–117.
63. Brandt, P.; Abson, D.J.; DellaSala, D.A.; Feller, R.; von Wehrden, H. Multifunctionality and biodiversity: Ecosystem services in temperate rainforests of the Pacific Northwest, USA. *Biol. Conserv.* **2014**, *169*, 362–371. [CrossRef]
64. Basuki, T.; van Laake, P.; Skidmore, A.; Hussin, Y. Allometric equations for estimating the above-ground biomass in tropical lowland Dipterocarp forests. *For. Ecol. Manag.* **2009**, *257*, 1684–1694. [CrossRef]
65. Patenaude, G.; Hill, R.; Milne, R.; Gaveau, D.; Briggs, B.; Dawson, T. Quantifying forest above ground carbon content using LiDAR remote sensing. *Remote Sens. Environ.* **2004**, *93*, 368–380. [CrossRef]
66. De Tanago, J.G.; Lau, A.; Bartholomeus, H.; Herold, M.; Avitabile, V.; Raumonen, P.; Martius, C.; Goodman, R.C.; Disney, M.; Manuri, S.; et al. Estimation of above-ground biomass of large tropical trees with terrestrial LiDAR. *Methods Ecol. Evol.* **2017**, *9*, 223–234. [CrossRef]
67. Calders, K.; Newnham, G.; Burt, A.; Murphy, S.; Raumonen, P.; Herold, M.; Culvenor, D.S.; Avitabile, V.; Disney, M.; Armston, J.D.; et al. Nondestructive estimates of above-ground biomass using terrestrial laser scanning. *Methods Ecol. Evol.* **2014**, *6*, 198–208. [CrossRef]
68. He, Q.; Chen, E.; An, R.; Li, Y. Above-ground biomass and biomass components estimation using LiDAR data in a coniferous forest. *Forests* **2013**, *4*, 984–1002. [CrossRef]
69. Brack, C.; Schaefer, M.; Jovanovic, T.; Crawford, D. Comparing terrestrial laser scanners' ability to measure tree height and diameter in a managed forest environment. *Aust. For.* **2020**, *83*, 161–171. [CrossRef]
70. Roussel, J.R.; Caspersen, J.; Béland, M.; Thomas, S.; Achim, A. Removing bias from LiDAR-based estimates of canopy height: Accounting for the effects of pulse density and footprint size. *Remote Sens. Environ.* **2017**, *198*, 1–16. [CrossRef]

71. Dassot, M.; Colin, A.; Santenoise, P.; Fournier, M.; Constant, T. Terrestrial laser scanning for measuring the solid wood volume, including branches, of adult standing trees in the forest environment. *Comput. Electron. Agric.* **2012**, *89*, 86–93. [CrossRef]
72. Astrup, R.; Ducey, M.J.; Granhus, A.; Ritter, T.; von Lüpke, N. Approaches for estimating stand-level volume using terrestrial laser scanning in a single-scan mode. *Can. J. For. Res.* **2014**, *44*, 666–676. [CrossRef]
73. Ducey, M.J.; Astrup, R.; Seifert, S.; Pretzsch, H.; Larson, B.C.; Coates, K.D. Comparison of forest attributes derived from two terrestrial lidar systems. *Photogramm. Eng. Remote Sens.* **2013**, *79*, 245–257. [CrossRef]
74. Giurgiu, V. *Dendrometrie și Auxologie Forestieră*; Ceres: Bucharest, Romania, 1979.
75. McVittie, A.; Hussain, S. The Economics of Ecosystems and Biodiversity—Valuation Database Manual. Available online: http://doc.teebweb.org/wp-content/uploads/2014/03/TEEB-Database-and-Valuation-Manual_2013.pdf (accessed on 1 March 2021).
76. Alamgir, M.; Turton, S.M.; Macgregor, C.J.; Pert, P.L. Assessing regulating and provisioning ecosystem services in a contrasting tropical forest landscape. *Ecol. Indic.* **2016**, *64*, 319–334. [CrossRef]
77. Burkhard, B.; Kroll, F.; Nedkov, S.; Müller, F. Mapping ecosystem service supply, demand and budgets. *Ecol. Indic.* **2012**, *21*, 17–29. [CrossRef]
78. De Groot, R.; Alkemade, R.; Braat, L.; Hein, L.; Willemen, L. Challenges in integrating the concept of ecosystem services and values in landscape planning, management and decision making. *Ecol. Complex.* **2010**, *7*, 260–272. [CrossRef]
79. Clark, P.J.; Evans, F.C. Distance to nearest neighbor as a measure of spatial relationships in populations. *Ecology* **1954**, *35*, 445–453. [CrossRef]
80. Vorčák, J.; Merganič, J.; Saniga, M. Structural diversity change and regeneration processes of the Norway spruce natural forest in Babia hora NNR in relation to altitude. *J. For. Sci.* **2012**, *52*, 399–409. [CrossRef]
81. Ajrhough, S.; Maanan, M.; Mharzi Alaoui, H.; Rhinane, H.; El Arabi, E.H. *Mapping Forest Ecosystem Services: A Review*; International Archives of the Photogrammetry, Remote Sensing and Spatial Information Science—ISPRS Archives; ISPRS: Hannover, Germany, 2019.
82. Houghton, R.A.; House, J.I.; Pongratz, J.; Van Der Werf, G.R.; Defries, R.S.; Hansen, M.C.; Le Quéré, C.; Ramankutty, N. Carbon emissions from land use and land-cover change. *Biogeosciences* **2012**, *9*, 5125–5142. [CrossRef]
83. Giurgiu, V.; Decei, I.; Draghiciu, D. *Metode si Tabele Dendrometrice*; Ceres: Bucharest, Romania, 2004.
84. Eggleston, S.; Buendia, L.; Miwa, K.; Ngara, T.; Tanabe, K. *Guidelines for National Greenhouse Gas Inventories: Agriculture, Forestry and Other Land Use*; IPCC: Hayama, Japan, 2006.
85. Lamlom, S.; Savidge, R. A reassessment of carbon content in wood: Variation within and between 41 North American species. *Biomass Bioenergy* **2003**, *25*, 381–388. [CrossRef]
86. Justine, M.F.; Yang, W.; Wu, F.; Tan, B.; Khan, M.N.; Zhao, Y. Biomass stock and carbon sequestration in a chronosequence of *pinus massoniana* plantations in the upper reaches of the Yangtze River. *Forests* **2015**, *6*, 3665–3682. [CrossRef]
87. Calders, K.; Schenkels, T.; Bartholomeus, H.; Armston, J.D.; Verbesselt, J.; Herold, M. Monitoring spring phenology with high temporal resolution terrestrial LiDAR measurements. *Agric. For. Meteorol.* **2015**, *203*, 158–168. [CrossRef]
88. Danson, F.; Hetherington, D.; Morsdorf, F.; Koetz, B.; Allgower, B. Forest canopy gap fraction from terrestrial laser scanning. *IEEE Geosci. Remote Sens. Lett.* **2007**, *4*, 157–160. [CrossRef]
89. Danson, F.M.; Morsdorf, F.; Koetz, B. Airborne and terrestrial laser scanning for measuring vegetation canopy structure. *Laser Scanning Environ. Sci.* **2009**, 201–219. [CrossRef]
90. Pascu, I.S.; Dobre, A.-C.; Zamfira, V.; Apostol, E.; Leca, Ș.; Pitar, D.; Apostol, B.; Chivulescu, Ș.; Ciceu, A.; Duro, J.G.; et al. Phenological analysis through the use of multitemporal TLS observations. *Rev. Silvic. Cineg.* **2020**, *XXV*, 38–45.
91. Jenkins, R.B. Airborne laser scanning for vegetation structure quantification in a south east Australian scrubby forest-woodland. *Austral. Ecol.* **2011**, *37*, 44–55. [CrossRef]
92. Savastru, D.M.; Zoran, M.A.; Savastru, R.S. Geospatial information for assessment of climate change impact on forest phenology. In *Seventh International Conference on Remote Sensing and Geoinformation of the Environment (RSCy2019)*; International Society for Optics and Photonics: Bellingham, WA, USA, 2019; Volume 11174, p. 1117402. [CrossRef]
93. Nezval, O.; Krejza, J.; Světlík, J.; Šigut, L.; Horáček, P. Comparison of traditional ground-based observations and digital remote sensing of phenological transitions in a floodplain forest. *Agric. For. Meteorol.* **2020**, *291*, 108079. [CrossRef]
94. Alivernini, A.; Fares, S.; Ferrara, C.; Chianucci, F. An objective image analysis method for estimation of canopy attributes from digital cover photography. *Trees* **2018**, *32*, 713–723. [CrossRef]
95. Stark, S.C.; Leitold, V.; Wu, J.; Hunter, M.; De Castilho, C.V.; Costa, F.R.C.; McMahon, S.M.; Parker, G.; Shimabukuro, M.T.; Lefsky, M.A.; et al. Amazon forest carbon dynamics predicted by profiles of canopy leaf area and light environment. *Ecol. Lett.* **2012**, *15*, 1406–1414. [CrossRef]
96. MacArthur, R.H.; Horn, H.S. Foliage profile by vertical measurements. *Ecology* **1969**, *50*, 802–804. [CrossRef]
97. Swinehart, D.F. The beer-lambert law. *J. Chem. Educ.* **1962**, *39*, 333. [CrossRef]
98. Calloway, D. Beer-lambert law. *J. Chem. Educ.* **1997**, *74*, 744. [CrossRef]
99. Sumida, A.; Nakai, T.; Yamada, M.; Ono, K.; Uemura, S.; Hara, T. Ground-based estimation of leaf area index and vertical distribution of leaf area density in a Betula ermanii forest. *Silva Fenn.* **2009**, *43*. [CrossRef]
100. Stark, S.C.; Enquist, B.; Saleska, S.R.; Leitold, V.; Schietti, J.; Longo, M.; Alves, L.; de Camargo, P.B.; Oliveira, R.C. Linking canopy leaf area and light environments with tree size distributions to explain Amazon forest demography. *Ecol. Lett.* **2015**, *18*, 636–645. [CrossRef]

101. Parker, G.G.; Harding, D.J.; Berger, M.L. A portable LIDAR system for rapid determination of forest canopy structure. *J. Appl. Ecol.* **2004**, *41*, 755–767. [CrossRef]
102. Kamoske, A.G.; Dahlin, K.M.; Stark, S.C.; Serbin, S.P. Leaf area density from airborne LiDAR: Comparing sensors and resolutions in a temperate broadleaf forest ecosystem. *For. Ecol. Manag.* **2018**, *433*, 364–375. [CrossRef]
103. Reid, W.V.; Mooney, H.A.; Cropper, A.; Capistrano, D.; Carpenter, S.R.; Chopra, K.; Zurek, M.B. *Ecosystems and Human Well-being-Synthesis: A Report of the Millennium Ecosystem Assessment*; Island Press: Washington, DC, USA, 2005.
104. Haines-Young, R.; Potschin, M. *CICES V5. 1. Guidance on the Application of the Revised Structure*; Fabis Consulting: Nottingham, UK, 2018.
105. Haines-Young, R.; Potschin, M. Common international classification of ecosystem services (CICES, Version 4.1). *Eur. Environ. Agency* **2012**, *33*, 107.
106. Li, S.; Wang, T.; Hou, Z.; Gong, Y.; Feng, L.; Ge, J. Harnessing terrestrial laser scanning to predict understory biomass in temperate mixed forests. *Ecol. Indic.* **2020**, *121*, 107011. [CrossRef]
107. Martire, S.; Castellani, V.; Sala, S. Carrying capacity assessment of forest resources: Enhancing environmental sustainability in energy production at local scale. *Resour. Conserv. Recycl.* **2015**, *94*, 11–20. [CrossRef]
108. Street, G.M.; Rodgers, A.R.; Avgar, T.; Fryxell, J.M. Characterizing demographic parameters across environmental gradients: A case study with Ontario moose (*Alces alces*). *Ecosphere* **2015**, *6*, art138. [CrossRef]
109. Pringle, R.M.; Fox-Dobbs, K. Coupling of canopy and understory food webs by ground-dwelling predators. *Ecol. Lett.* **2008**, *11*, 1328–1337. [CrossRef]
110. Arnold, J.M.; Gerhardt, P.; Steyaert, S.M.; Hochbichler, E.; Hackländer, K. Diversionary feeding can reduce red deer habitat selection pressure on vulnerable forest stands, but is not a panacea for red deer damage. *For. Ecol. Manag.* **2018**, *407*, 166–173. [CrossRef]
111. Ewald, M.; Dupke, C.; Heurich, M.; Muller, J.P.; Reineking, B. LiDAR remote sensing of forest structure and GPS telemetry data provide insights on winter habitat selection of european roe deer. *Forests* **2014**, *5*, 1374–1390. [CrossRef]
112. Martinuzzi, S.; Vierling, L.A.; Gould, W.A.; Falkowski, M.J.; Evans, J.S.; Hudak, A.T.; Vierling, K.T. Mapping snags and understory shrubs for a LiDAR-based assessment of wildlife habitat suitability. *Remote Sens. Environ.* **2009**, *113*, 2533–2546. [CrossRef]
113. Nilsson, M.-C.; Wardle, D.A. Understory vegetation as a forest ecosystem driver: Evidence from the northern Swedish boreal forest. *Front. Ecol. Environ.* **2005**, *3*, 421–428. [CrossRef]
114. Gilliam, F. The ecological significance of the herbaceous layer in temperate forest ecosystems. *BioScience* **2007**, *57*, 845–858. [CrossRef]
115. Hill, R.; Broughton, R. Mapping the understorey of deciduous woodland from leaf-on and leaf-off airborne LiDAR data: A case study in lowland Britain. *ISPRS J. Photogramm. Remote Sens.* **2009**, *64*, 223–233. [CrossRef]
116. Gersom, Z. *Mapping the Shrub Layer in a Forest Using LiDAR*; Wageningen University and Research Centre: Wageningen, The Netherlands, 2018.
117. Wing, B.M.; Ritchie, M.W.; Boston, K.; Cohen, W.B.; Olsen, M.J. Individual snag detection using neighborhood attribute filtered airborne lidar data. *Remote Sens. Environ.* **2015**, *163*, 165–179. [CrossRef]
118. Tallis, H.; Ricketts, T.H.; Daily, G.C.; Polasky, S. Natural Capital: Theory and Practice of Mapping Ecosystem Services—Oxford Scholarship. Available online: https://www.amazon.com/Natural-Capital-Practice-Ecosystem-Services/dp/0199589003 (accessed on 1 March 2021).
119. Maes, J.; Crossman, N.D.; Burkhard, B. Mapping ecosystem services. In *Handbook of Ecosystem Services*; Routledge: London, UK, 2018.
120. Lautenbach, S.; Kugel, C.; Lausch, A.; Seppelt, R. Analysis of historic changes in regional ecosystem service provisioning using land use data. *Ecol. Indic.* **2011**, *11*, 676–687. [CrossRef]
121. Martin, M.; Newman, S.; Aber, J.; Congalton, R. Determining forest species composition using high spectral resolution remote sensing data. *Remote Sens. Environ.* **1998**, *65*, 249–254. [CrossRef]
122. Ørka, H.O.; Dalponte, M.; Gobakken, T.; Næsset, E.; Ene, L.T. Characterizing forest species composition using multiple remote sensing data sources and inventory approaches. *Scand. J. For. Res.* **2013**, *28*, 677–688. [CrossRef]
123. Penman, J.; Gytarsky, M.; Hiraishi, T.; Irving, W.; Krug, T. *Guidelines for National Greenhouse Gas Inventories*; IPCC: Geneva, Switzerland, 2006.
124. Pandey, R. Indices for measuring forest ecosystem goods and services contribution to the rural community: A tool for informed decisions. *J. Environ. Prof. Sri Lanka* **2013**, *1*, 58. [CrossRef]
125. Czúcz, B.; Haines-Young, R.; Kiss, M.; Bereczki, K.; Kertész, M.; Vári, Á.; Potschin-Young, M.; Arany, I. Ecosystem service indicators along the cascade: How do assessment and mapping studies position their indicators? *Ecol. Indic.* **2020**, *118*, 106729. [CrossRef]
126. Burkhard, B.; Santos-Martín, F.; Nedkov, S.; Maes, J. An operational framework for integrated Mapping and Assessment of Ecosystems and their Services (MAES). *One Ecosyst.* **2018**, *3*, e22831. [CrossRef]
127. Song, Z.; Seitz, S.; Li, J.; Goebes, P.; Schmidt, K.; Kühn, P.; Shi, X.; Scholten, T. Tree diversity reduced soil erosion by affecting tree canopy and biological soil crust development in a subtropical forest experiment. *For. Ecol. Manag.* **2019**, *444*, 69–77. [CrossRef]
128. Loustau, D.; Granier, A.; Bréda, N. A generic model of forest canopy conductance dependent on climate, soil water availability and leaf area index. *Ann. For. Sci.* **2000**, *57*, 755–765. [CrossRef]

129. Manes, F.; Marando, F.; Capotorti, G.; Blasi, C.; Salvatori, E.; Fusaro, L.; Ciancarella, L.; Mircea, M.; Marchetti, M.; Chirici, G.; et al. Regulating ecosystem services of forests in ten Italian metropolitan cities: Air quality improvement by PM10 and O3 removal. *Ecol. Indic.* **2016**, *67*, 425–440. [CrossRef]
130. Bobiec, A. Living stands and dead wood in the Białowieża forest: Suggestions for restoration management. *For. Ecol. Manag.* **2002**, *165*, 125–140. [CrossRef]